

Wright State University

CORE Scholar

[Browse all Theses and Dissertations](#)

[Theses and Dissertations](#)

2015

Connectivity of Monosynaptic Ia afferents on Renshaw Cells in Neonatal Mice

Todd Joseph Rapetti
Wright State University

Follow this and additional works at: https://corescholar.libraries.wright.edu/etd_all



Part of the [Anatomy Commons](#)

Repository Citation

Rapetti, Todd Joseph, "Connectivity of Monosynaptic Ia afferents on Renshaw Cells in Neonatal Mice" (2015). *Browse all Theses and Dissertations*. 1404.
https://corescholar.libraries.wright.edu/etd_all/1404

This Thesis is brought to you for free and open access by the Theses and Dissertations at CORE Scholar. It has been accepted for inclusion in Browse all Theses and Dissertations by an authorized administrator of CORE Scholar. For more information, please contact library-corescholar@wright.edu.

CONNECTIVITY OF MONOSYNAPTIC IA
AFFERENTS ON RENSCHAW CELLS IN
NEONATAL MICE

A thesis submitted in partial fulfillment of the
Requirements for the degree of
Master of Science

By

TODD JOSEPH RAPETTI
B.A., Miami University, 2002

2015
Wright State University

WRIGHT STATE UNIVERSITY

GRADUATE SCHOOL

JULY 8, 2015

I HEREBY RECOMMEND THAT THE THESIS PREPARED UNDER MY SUPERVISION BY Todd Joseph Rapetti ENTITLED Connectivity of Monosynaptic Ia Afferents on Renshaw Cells in Neonatal Mice BE ACCEPTED IN PARTIAL FULFILLMENT OF THE REQUIREMENTS FOR THE DEGREE OF Master of Science.

David Ladle, Ph.D.
Thesis Director

Christopher N. Wyatt, Ph.D.
Interim Department Chair
Department of Neuroscience, Cell Biology
and Physiology

Committee on
Final Examination

Larry Ream, Ph.D.

Patrick Sonner, Ph.D.

Robert E. W. Fyffe, Ph.D.
Vice President for Research and
Dean of the Graduate School

ABSTRACT

Rapetti, Todd Joseph. M.S. Department of Neuroscience, Cell Biology, and Physiology, Wright State University, 2015. Connectivity of Monosynaptic Ia Afferents on Renshaw Cells in Neonatal Mice

Proprioception allows sensory information about muscle position and length to enter the CNS without the aid of visual cues. One type of fiber that carries this information is the Ia afferent, which innervates muscle spindles that respond to mechanical perturbation in muscle. Ia fibers are known to synapse with Ia interneurons (INs) and motor neurons (MNs), setting up important circuits which affect movement. Another type of IN is the Renshaw cell (RC), which is located in the ventral part of lamina VII of the spinal cord and is critical for the functionality of the recurrent inhibitory circuit. In addition to sending inhibitory axons to MNs, RCs were recently discovered to receive monosynaptic Ia afferent connections. Sensory connections increase from birth through postnatal day (P) 15 in a mouse model, and then decline functionally into adulthood. The functional relevance and possible muscle-specific patterns of sensory connectivity with RCs is poorly understood. To investigate this question, we mapped the connections of proprioceptive afferents of quadriceps and obturator nerves (with fluorescent dextran retrograde tracing) onto immunohistochemically defined RCs in neonatal mice (P0 or P1). We hypothesized

the quadriceps and obturator afferents would contact different populations of RCs, implying selective activation. Our results indicate RCs are almost twice as likely to receive obturator sensory contacts as quad contacts at this stage, and that there is a population of RCs which receive contacts from both types of afferents. A possible explanation is that synaptic contact patterns may change in the course of postnatal development to eliminate convergent inputs from both types of afferents. Alternatively, all RCs may be contacted by afferents from various muscle nerves to allow for generalized feedforward inhibition during early postnatal development.

TABLE OF CONTENTS

	Page
I. INTRODUCTION.....	1
General Anatomy of the Spinal Cord.....	1
Spinal Cord Circuitry.....	2
Renshaw Cells, Recurrent Inhibition, and Physiology.....	3
Development of RCs.....	5
Development of Interneuronal Circuits.....	6
Development of Proprioceptive Afferents.....	7
Monosynaptic Ia Afferent Connections with RCs.....	8
II. METHODS.....	11
Preparation and quadriceps and obturator nerve tracing.....	11
Immunohistochemistry.....	13
Confocal Imaging and Spot Scope.....	15
Image Analysis.....	15
III. RESULTS.....	19
IV. DISCUSSION.....	45
V. BIBLIOGRAPHY.....	54

LIST OF FIGURES

Figure	Page
1. Immunohistochemical 20X image panel of P0/P1 hemisected spinal cord.....	21
2. Distribution of obturator and quad afferents in the RC area of segments L3/L4 around the rostrocaudal axis.....	27
3. Immunohistochemical image panel of L4 DRG neurons of the quadriceps and obturator nerves.....	31
4. Types of RC populations.....	35
5. Immunohistochemical 60X image panel showing possible contact types.....	37
6. Average percent of RCs with Different Types of Contact for 5 Animals.....	41

LIST OF TABLES

Table	Page
1. Antibodies used in this study.....	18
2. Number of CB+ cells in the RC area and total length of cord examined (um) for 5 animals.....	23
3. Number of total L3/L4 DRG neurons for the quad and obturator nerves in 5 animals.....	29
4. Cell Contact Data for obturator and quad nerves in the RC area.....	39
5. Average number of contacts/cell and the range for 5 animals.....	43

I. INTRODUCTION

General Anatomy of the Spinal Cord

The spinal cord is a main component of the central nervous system, and is critically important for receiving and integrating sensory information from the periphery, as well as sending motor output to skeletal muscle. The spinal cord is divided between the white matter, which forms the exterior, and the gray matter in the interior. The white matter consists of groups of myelinated nerve cell processes (axons) called tracts, which relay information to and from the brainstem and cerebrum. For example, the corticospinal tract carries efferent information from the primary motor cortex, through the brainstem and is processed in the spinal cord. Eventually, this information is relayed to muscle for production of voluntary movement. The gray matter consists of neuronal cell bodies, and in the spinal cord it is broken up into three main areas—the ventral horn, lateral horn, and dorsal horn. The ventral horn contains motor neurons and processes motor output, the lateral horn mainly contributes to the sympathetic portion of the autonomic nervous system, while the dorsal horn is generally responsible for processing incoming sensory information. All three horns contain interneurons, which act as mediators between neurons that are motor or sensory. The three horns of the spinal cord are further broken up into ten different laminae, with laminae I-VI

located in the dorsal horn, part of lamina VII and lamina X in the lateral or intermediate horn, and part of lamina VII and laminae VIII and IX in the ventral horn. The different laminae are organized by the type and function of neurons in a certain location, or more specifically their physiological, histochemical, and cytoarchitectonic properties (Sengul et al., 2012). This thesis is focused on the ventral-most portion of laminae VII and IX; lamina IX contains motorneurons (MNs), and lamina VII has a specific type of interneuron (IN) that is of particular interest.

Spinal Cord Circuitry

All of the sensory information that is entering the spinal cord is transduced into an electrical signal via various somatosensory receptors located throughout the body. The different modalities of receptor type include but are not limited to thermoreception, mechanoreception, nociception, and proprioception. Proprioception allows us to be aware of our body's position in space and the amount of force being used on our muscles during movement without the aid of visual cues. This is partially accomplished through proprioceptors called muscle spindles, which are located in the body of a muscle and detect changes in muscle length. Muscle spindles are innervated by Ia afferents and group II afferents, fibers which enter the spinal cord through the dorsal root entry zone and make projections to the ventral horn. Group Ia afferents make connections with MNs and Ia INs in the ventral horn (Wang et al., 2008), and are integral to the monosynaptic stretch reflex and reciprocal inhibition, respectively. The monosynaptic stretch reflex and reciprocal inhibition are types of spinal cord circuits, which essentially consist of neurons that are interconnected and fire together to produce an action in

muscles. For example, when a muscle is stretched, Ia afferents innervating muscle spindles activate MNs in the ventral horn which then project to homonymous or synergistic muscles. These muscles then produce a contraction to oppose the stretch, thus termed the “monosynaptic stretch reflex” (Chen et al., 2003). Reciprocal inhibition is a little more complicated because it is disynaptic, and the Ia afferents from a flexor muscle first synapse with Ia inhibitory INs. This IN then decreases the firing rate of the extensor MN, thus preventing the extensor muscle from contracting at the same time as the flexor muscle. From these two examples, it is clear that spinal cord circuits are an essential aspect of proper motor function.

Renshaw Cells, Recurrent Inhibition, and Physiology

Another important circuit in the spinal cord is recurrent inhibition. This is mediated by a type of IN called a Renshaw cell (RC), which is the focus of this study. RCs are located in proximity to MNs in the ventral portion of laminae VII and IX. They are excited by alpha MN (MN's that innervate extrafusal muscle fibers of skeletal muscle and cause contraction) axon collaterals, and send inhibitory projections to homonymous and synergistic MNs (Alvarez et al., 2013), providing a negative feedback loop. This inhibition of MNs via RCs is a powerful one, because there is a lot of neurotransmitter release sites on the MNs, mainly their dendrites (Bhumbra et al., 2014). In fact, a single RC is capable of inducing a significantly lower MN firing rate (Bhumbra et al., 2014). Because the alpha MN is now firing less, over-activity of the muscle is prevented. Thus, RCs are integral to coordination of motor activity (Bhumbra et al., 2014).

The circuitry and physiology of RCs are more complicated than just a simple negative feedback loop. RCs are known to inhibit antagonistic RCs, inhibit IaINs, and receive descending information from the brain (Alvarez and Fyffe, 2007). During in vivo electrophysiology experiments, when MNs are excited to evoke motor activity, RCs receive simultaneous inhibitory inputs from inhibitory INs other than RCs, and the degree of inhibition is proportional to the amount of excitatory inputs to MNs (Nishimaru et al., 2010). This is presumably a way of decreasing RC inhibition on active MNs, and this type of RC modulation is an important factor when considering how motor output is controlled in the spinal cord (Nishimaru et al., 2010). It has also been shown that according to the frequency range, RC action varies (Williams and Baker, 2009). For example, when RCs are set at a 10 Hz frequency using a biophysical computational model, synchronous oscillations are sent back to MNs which leads to inhibition of MN firing (recurrent inhibition) (Williams and Baker, 2009). Using this same model, setting the RCs at 30 Hz actually increases MN activity (Williams and Baker, 2009). Because physiological tremor has been shown to occur when MNs are firing at 10 Hz oscillations, the RC feedback loop can aid in diminishing the severity of physiological tremor.

Interestingly, RC inhibition is greater on motor pools that innervate proximal musculature (more ventrally located motor neurons) than distal musculature (more dorsally located motor pools) (Alvarez et al., 2005); so, RC's indirectly exert more of an effect on trunk muscles than on muscles of the digits. RCs mainly affect MNs which innervate neck muscles, proximal limb muscles (excluding digits), and the diaphragm (Bhumbra et al., 2014).

Development of RCs

Regarding development of RCs, they all stem from V1 INs, a type of embryonic post-mitotic IN. There are three other classes of embryonic INs (V0, V2, V3) that differentiate into premotor INs in the ventral horn (Siembab et al., 2010). All four of these embryonic INs arise from progenitor cells P0, P1, P2, or P3 that are each located in a specific domain in the developing ventral spinal cord (Siembab et al., 2010). Approximately 9% of V1 INs become RCs, 13% become IaINs, and the vast majority develop into unknown types of INs (Alvarez et al., 2005). V1 INs are divided into early and late maturation groups, with RC's fitting the early category and IaINs developing later (Benito-Gonzalez and Alvarez, 2012); this early phase corresponds from E9.5 to E10.5, the time when RCs are born (Alvarez et al., 2005). V1 interneurons are inhibitory in nature, originate in the p1 progenitor area, and eventually migrate ventrolaterally to become positioned adjacent to motor pools. These motor neurons are then targeted by growing axons of the V1 interneurons (Siembab et al., 2010). Thus, V1 interneurons are positioned close to MNs, providing an important relationship between anatomical location and function.

Various transcription factors are necessary for the development of V1 INs and eventually RCs. For example, V1 interneurons develop from Pax6+/Nkx6.2+/Dbx2+ progenitors. In Pax6 gene knockout mice, RC's are absent, which proves that Pax6 is necessary for RC differentiation (Sapir et al., 2004). Pax6 is integral to normal development of RC's, however the Pax6 gene is not required for IaIN formation (Wang et al., 2008)—this shows that Pax6 is selective for specific types of V1 interneurons (i.e., RCs).

Pax6 is required for RC formation, but other transcription factors affect RC development differently at various stages. For example, En1 is expressed by V1 INs, and En1 mutants have the same number of RC's as wild type, however there are less inhibitory connections with MNs (Sapir et al., 2004). Thus, the recurrent inhibitory circuit would be impacted. Alternatively, MafB is not necessary for the development of the recurrent inhibitory circuit, however, it is needed for RCs to express calbindin (a calcium binding protein that is a marker for RCs along with anatomical location) and for RCs to stay functional (Stam et al., 2012); consequently, MafB is required for the maintenance of RCs. Oc1/Oc2 transcription factors are also needed for RCs to continue to express MafB and calbindin after Foxd3 initiates their expression in developing RCs (Stam et al., 2012). So, in the absence of Oc1 and Oc2, Calbindin will not be present to bind calcium, and RCs will not function properly at the synaptic level. Also, Foxd3 is required for RCs to develop after their fate has been determined postmitotically (Stam et al., 2012). In addition, RCs can begin to differentiate when Oc1 and Oc2 are not present, however after E12.5, RC numbers wane as the developmental process becomes interrupted (Stam et al., 2012); thus, Oc1/Oc2 are also required for early RC development. Overall, various transcription factors are responsible for the formation of different interneurons (i.e., RCs) and their inclusion into spinal circuits that control movement.

Development of Interneuronal Circuits

There are four discrete phases in the development of interneuronal circuits (Alvarez et al., 2013). The first step is that specific genes encode for various interneurons at the progenitor level. An example of this is the Pax-6 gene being a

necessity for RC formation. Secondly, connectivity is determined based on information about position and targets of growing axons. For example, En1 is a requirement for the targeting of inhibitory RC connections with MNs. The third step is that synaptogenesis occurs separately from neuronal activity. For instance, the recurrent inhibitory circuit formation does not require synaptic activity (Alvarez et al., 2013). Lastly, after birth, synapses eventually mature in an activity-dependent manner. An example of this is the alteration of different inputs which affect RC activity as the animal reaches adulthood. Interestingly, even in the absence of neural activity, RCs still form synapses with motor neurons, albeit with less organization—this implies that activity may refine these connections, and thus be an integral component in setting up the proper recurrent inhibition pathways necessary for motor function (Stam et al., 2012). In summary, before birth, there is strong organization and input selectivity on interneurons, and strengthening or weakening of these synapses occurs postnatally which can result in significant circuit changes (Siembab et al., 2010).

Development of Proprioceptive Afferents

Similar to development of RCs and interneuronal circuits, development of proprioceptive afferents and their innervation of muscle spindles are also a complicated process involving numerous transcription and growth factors. Ia proprioceptive afferents fail to develop properly in ER81 mutant mice and do not make it to the ventral horn to supply MNs. Instead, the afferents will terminate in the lateral horn. The nerve growth factor NT3 induces expression of ER81 in Ia afferents (Patel et al., 2003). Thus, Ia afferent projections do not form in mice

deficient of NT3, and neither do IaINs (Kucera et al., 1995). NT3 also affects circuit formation, because elevated NT3 causes disruption in the development of the stretch reflex circuit (Wang et al., 2007). The receptor for NT3 is TrkC, and so it follows that this receptor is also needed for proprioceptive sensory neurons to stay alive (Chen et al., 2003). Muscle spindles provide an important peripheral source of NT3 during postnatal development. In *Egr3* knockout mice, muscle spindle function is lost, thus decreasing NT3—this leads to decreased firing of MNs when stimulated by proprioceptive sensory afferents (Chen et al., 2002).

In addition to ER81 and its associated proteins, cell-adhesion molecules F11 and NrCAM are necessary for Ia afferents to make their proper terminations in the ventral horn (Chen et al., 2003). Another important transcription factor is Runx3, which is integral to differentiation and proper connectivity of Ia afferents (Chen et al., 2006). As far as Ia afferent connectivity with MNs is concerned, Ia afferents that express *Wnt3* help these afferents branch to their MN targets (Chen et al., 2003). Also, synapse formation between MNs and Ia afferents may be mediated by cadherins, a type of cell-surface protein (Chen et al., 2003).

Monosynaptic Ia Afferent Connections with RCs

Because we know that Ia afferents develop projections to the ventral horn and make connections with MNs, do Ia afferents form direct synapses with RCs? When RCs were first discovered, it was shown that activating dorsal roots stimulate RCs (Renshaw, 1946). This was later explained by way of the monosynaptic stretch reflex: when MNs are discharged by the afferents, the MN collaterals are secondarily activated and RCs are excited (Eccles et al., 1954). Thus, it was believed

for a very long time that there were no direct sensory connections with RCs. Several years later it was shown that this statement is indeed false.

It has been demonstrated via dorsal root fills that there are monosynaptic sensory neuron connections with RC's in newborns to age P15, but that they lose functionality in adulthood (Mentis et al., 2006). Adult-like locomotion occurs around P15, coinciding with a functional decline of monosynaptic afferent connections on RC's and stabilization of motor synapses with RC's (Siembab et al., 2010). These sensory synapses were identified with vesicular glutamate transporter 1 (VGLUT1), a presynaptic marker, and the motor axon synapses were identified with vesicular acetylcholine transporter (VAcHT). Thus, from birth until P15 there is an increasing number of RCs with monosynaptic afferent inputs, as every RC in the L4/L5 area received primary afferent contact by P10 (Mentis et al., 2006). These primary afferents are most likely Ia afferents, due to the ventral location of the RCs (Mentis et al., 2006). In addition to providing anatomical evidence of monosynaptic Ia afferent connections with RCs, it was also proved that these connections are functional via electrophysiological studies (Mentis et al., 2006).

The aim of this thesis is to further study these Ia afferent contacts with RCs and gain a better understanding of the development, connectivity pattern, and anatomy of the connections. Mentis et al. (2006) performed backfills on dorsal root L5, so in order to expand upon this work, the connectivity of afferents from different muscles during development will be examined. This will be accomplished by using a spinal cord preparation of newborn mice, where two different nerves that supply

different muscles will be backfilled. Specifically, we will use the quadriceps and obturator nerves. These nerves provide a good model because they innervate different muscles that act on separate joints and have different actions. Also, their afferent cells are in the same DRGs and their axons enter the same dorsal roots, so their neuronal connections with RCs in the ventral horn can easily be compared. Importantly, the quadriceps nerve innervates only quadriceps MNs, and the obturator nerve innervates only obturator MNs. Thus, we can see from these studies if the same pattern holds true with afferent connections on RCs. In addition to specific nerve fills, immunohistochemistry will be performed so that the connectivity pattern of Ia afferents on RCs can be examined. I hypothesize that Ia afferents from quad/obturator nerves will contact a separate population of RC's in non-overlapping clusters in the ventral part of lamina VII and IX at birth (P0 or P1). This would suggest that the connectivity pattern is leading to a specific function during murine development.

II. MATERIALS AND METHODS

All animal experimental procedures were conducted under the approval of the Wright State University Laboratory Animal Care and Use Committee.

Preparation and quadriceps and obturator nerve tracing

Fluorescent dextrans (Invitrogen) were used to trace sensory afferents of wild type (WT) mice (age P0 or P1) from the quadriceps and obturator nerves to their terminations in the spinal cord. The animal was anesthetized via hypothermia in an ice cold water bath for approximately 2 minutes. It was then pinned in a dish with a Sylgard base and the thoracic cavity was exposed. This allowed access to the heart and the left ventricle, where 5 ml of ice cold oxygenated artificial cerebrospinal fluid (ACSF) was transcardially perfused with a 5 ml syringe bearing a 27 gauge needle. The ACSF consisted of 127 mM of NaCl, 1.9mM of KCl, 1.2 mM KH₂PO₄, 1 mM MgSO₄ * 7H₂O, 26 mM NaHCO₃, 16.9 D(+)glucose monohydrate, and 500 µl of CaCl₂ was added to this solution after it was bubbled in oxygen for a minimum of 15 min. This solution was continually oxygenated throughout the duration of the experiment.

The animal was decapitated, and the organs eviscerated. The skin was removed over the dorsal aspect of the mouse to ensure adequate access to the

vertebrae. The left hind limb was removed at the hip joint as well as the tail. The prep was transferred to a chamber, also with a Sylgard base, that allows continual flow of the cold oxygenated ACSF via a pump (ThermoScientific) to keep the neurons in the spinal cord alive. A dorsal laminectomy was then performed to expose the spinal cord, roots, and DRGs. The dura mater over the spinal cord was also removed. Next, the cord was hemisected longitudinally because only the right side is needed, and it allows more efficient perfusion. The dorsal roots of the thoracic and sacral cord were cut to free up the cord, and the lumbar dorsal roots (especially L3/L4) were kept intact. All ventral roots were cut because we only want the dextrans to trace the sensory afferents, not the motor axons. To finish the prep, various leg and vertebral column muscles and connective tissue were cut away to expose the quadriceps and obturator nerves on the animals' right side.

The two nerves were then cut free and fitted with glass pipettes from World Precision Instruments Inc. (4 inch thinwall glass; 1.2mm OD/0.9mm ID), and shaped to the proper size of the nerves via fire polishing. Manipulators were utilized to correctly place the pipette near the nerves, and the nerves were suctioned into the glass capillaries. Next, the ACSF was withdrawn from the pipette and a solution (2.5 μ l) of fluorescently labeled dextran was added. In order to visualize the quad nerve, Tetramethylrhodamine dextran (3000 MW; Invitrogen [cat. no. D3308] was used, and for the obturator nerve, biotinylated dextran amine (BDA, 3000 MW; Invitrogen [cat no. D-7135]) was utilized. To allow the axons of these afferent nerves to be properly retrogradely transported and reach the ventral horn, the glass pipettes were left on the nerves for 19 hours. To maintain a temperature of about 30°C in

the dissection chamber, the oxygenated ACSF was placed on a hot plate during this time period. The quality of retrograde transport and axon labeling was checked using an Olympus MVX10 fluorescent dissecting stereomicroscope, and the specimen was then placed in 4% paraformaldehyde fix for 24 hrs. After being in fix for a day, the prep was cryoprotected by immersion into a 30% sucrose solution for a minimum of 24 hours, until ready to be sectioned.

Once ready for sectioning, the spinal cord was again viewed under the fluorescent stereomicroscope and a segment of cord where axons were labeled most vibrantly with tetramethylrhodamine, corresponding to approximately L3 and L4, was removed. In addition, L3 and L4 DRGs were cut out along with their attached bone. These sections of tissue were then embedded in O.C.T. Embedding Compound (TissueTek; # 4583, Electron Microscopy Sciences) and frozen in -80°C for at least 45 min. The tissue was then brought to an optimal cutting temperature by being placed in the Thermo Scientific HM 550 cryostat at around -30° for 45 min. Keeping with this temperature, the tissue was mounted and cut into $20\ \mu\text{m}$ thick sections using the cryostat. Both spinal cord and DRG sections were placed on Fisherbrand Superfrost Plus microscope slides, and organized into 3 or 4 series for each tissue.

Immunohistochemistry

Sections on the slides to be stained were first outlined with a hydrophobic pen (Aqua Hold II Barrier Pap Pen, Scientific Device Laboratories) in order to keep the antibody solution on top of the sections. Slides were next washed 3X for 5 min in 1X PBS. Blocking buffer was made so the antibody only binds the antigen of

interest. (PBS, 1 % BSA (Fisher Scientific), 0.1% Triton detergent solution). There were 3 different primary antibodies and 3 different secondary antibodies used for the experiments, and they were mixed at the proper working dilution with the blocking buffer solution. The first primary used was rabbit α -tetramethylrhodamine (Life Tech, 1:5000) in order to enhance the rhodamine backfill signal. Mouse α -biotin (Jackson IR, 1:1000) amplified the BDA backfill signal. Finally, for the primaries, goat α -Calbindin (Santa Cruz Biotech, 1:500) was utilized. The secondary antibodies were donkey α -rabbit (Jackson IR, 1:1000), donkey α -mouse (Jackson IR, 1:1000), and donkey α -goat (Jackson IR, 1:100). They were each conjugated to the following fluorophores, respectively: Cy3 (quad nerve), Alexa 488 (FITC; obturator nerve), and Alexa 647 (Cy5; Cablbin/RCS). All of the antibodies used are listed in Table 1. The primary antibodies were centrifuged (Eppendorf 5415D) and added to the chosen amount of blocking buffer solution to meet the proper working dilution. This entire solution was mixed by a Fisher Scientific Vortex Mixer, distributed on the slides, and left overnight at 4°C. The following day, slides were washed 3X 5 min in 1X PBS, and secondary antibodies were prepared the same way, except for a filtering step after the antibodies were added to the blocking buffer. The solution was captured with a syringe and passed through a Millex-GV 0.22 μ m Filter Unit to purify the secondary antibody solution. This solution was placed on the sections for 45 min at room temperature and then washed 3X 5 min in 1X PBS. Finally, the slides were cover-slipped using Vectashield mounting Medium (Vector Laboratories) and VWR micro cover glass.

Confocal Imaging and Spot Scope

The stained sections were imaged via an Olympus FV1000 confocal microscope. 488 nm, 568 nm, and 633 nm lasers were utilized to view the BDA, tetramethylrhodamine, and calbindin, respectively. There were around 3 series for each animal, and 1 series was imaged per animal, thus each section was approximately 60 μm apart. 20X images were taken of the entire section to view the calbindin position and obtain a reference point for the higher magnification 60X images. The 20x image stack was taken with a 1 μm z-step size. 60X objectives were used to obtain image stacks of Renshaw cells and the axons using all 3 lasers. These images were taken with a 0.3 μm z-step size and were set at a 2.5X optical zoom. PMT values were set accordingly to prevent oversaturation of the image, as was laser intensity to maximize signal brightness while preventing bleaching of the tissue. The 60X image stacks allowed us to acquire data in 3 channels for quantification of quad and obturator contacts on RCs using the Imaris analysis software. For the DRG cell counts, an Olympus Epi Fluorescence Scope with RT Spot color camera was used. Obturator sensory DRG neurons were counted manually through the 20X objective using the FITC channel, and the quad sensory DRG neurons were counted in the same way using the Cy3 channel.

Image Analysis

Images were analyzed using the Imaris x64 7.6.5 software. The contacts on individual cells under 60X magnification were assessed using the Ortho Slicer under the surpass mode. The Ortho Slicer allowed us to go through each individual slice in

the z-stack, to see if an obturator or quad contact occurred on the RC. The brightness and contrast of the signals were changed in each channel to better visualize possible contacts, without actually creating a false signal (altering the gamma level). If there was a contact in a certain plane, the position was noted. In addition, the number of contacts on a specific cell were noted. The cell was included as having an obturator, quad, or both types of contact if one or more contact was present on the soma or dendrites.

Table 1. Antibodies used in this study.

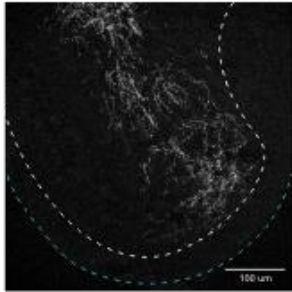
Antigen	Host/Type	Manufacturer	Specificity	Dilution	Catalogue #	Lot #
Tetramethyl-rhodamine	Rabbit Polyclonal	Invitrogen	Detects the Rhodamine Red Fluorophore	1:5000	A6397	430232
Biotin	Mouse Polyclonal	Jackson IR	Detects the BDA blue Fluorophore	1:1000	200-002-211	92972
Calbindin	Goat Polyclonal	Santa Cruz Biotech	Detects a single band of calbindin D-28K	1:500	sc-7691	E0514
Anti-rabbit Cy3 Fluorophore	Donkey	Jackson IR	Reacts with whole molecule Rabbit IgG	1:1000	711-165-152	110864
Anti-mouse Alexa Fluor 488	Donkey	Jackson IR	Reacts with whole molecule Mouse IgG	1:1000	715-545-151	114474
Anti-goat Alexa Fluor 647	Donkey	Jackson IR	Reacts with whole molecule Goat IgG	1:100	705-605-003	98917

II. RESULTS

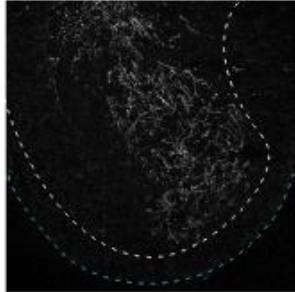
Retrograde tracing was performed on quadriceps and obturator Ia afferents to compare and examine their connectivity pattern with RCs in P0 and P1 mice. RCs were classified based on calbindin (CB) immunoreactivity and anatomical location. CB+ cells were only counted as a RC if they were located in the RC area (Fig. 1). The RC area is basically defined as the ventral-most area of the ventral horn adjacent to the white matter border, and medial to the lateral MNs (yellow box in Fig. 1). In addition, in P18 mice, the Renshaw cell area is defined as a CB+ cell within 200 μm dorsal from the white matter border in laminas VII and IX (Sapir et al., 2004). For our purposes, in P0 and P1 mice with smaller cords, we were conservative in defining our RCs as being within 100 μm from the white matter border and lateral to the midline of the hemisected cord (yellow box in Fig. 1). Also in Figure 1, the red fluorescence illustrates quadriceps axons in the Cy3 channel, and the green fluorescence illustrates obturator axons in the FITC channel. Actual connectivity on RCs was not able to be examined until higher magnification images were taken. The raw count of CB+ cells located in our defined RC area for 5 animals ranged from 35-86, and total length of cord examined ranged from 900-1740 μm , as seen in Table 2. This variation was due to estimating the length of cord where the axons are labeled with the dissection microscope, and cutting the cord based on this visual estimation.

Figure 1. Immunohistochemical 20X image panel of P0/P1 hemisected spinal cord. Merge shows green fluorescence as obturator afferents, red fluorescence as quad afferents, and Calbindin+ cells in grey. Blue dashed line indicates border of the cord, white dashed line is white matter border. Arrowheads indicate Renshaw Cells. Yellow box is approximate RC area. Scale bar 100 um.

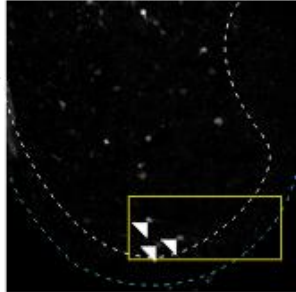
Quad Aff. (Rhodamine)



Obt Aff. (BDA)



Calbindin



Merge

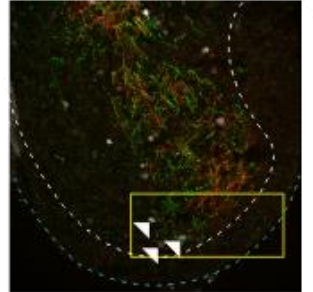


Table 2. Number of CB+ cells in the RC area and total length of cord examined (um) for 5 animals.

Number of CB+ cells in the RC area and total length of cord examined (um) for 5 animals.

Animal Number	Total Calbindin + Cells in RC Area	Total Length of Cord Examined (um)
1	35	1140
2	45	900
3	59	1260
4	57	1620
5	86	1740

Also from 20X images, we were able to ascertain the length of cord with only obturator afferents in the RC area, only quadriceps afferents in the RC area, or both obturator and quadriceps afferents in the RC area (Fig. 2). This allowed us to separate the data, with the majority of the data coming from where the two types of axons are both present in the RC area. In fact, only the obturator afferents occurred in the RC area at places in the spinal cord where quadriceps afferents did not. Thus, obturator afferents were present in the RC area for a longer length of cord than the quad afferents for all five animals. This could have occurred either rostral or caudal to the part of the cord where quad afferents were present in the RC area, as seen in Figure 2.

To evaluate the quality of afferent labeling, dorsal root ganglion (DRG) sections were also stained. From these sections, the number of labeled sensory neurons could be determined. The number of labeled quadriceps neurons (Cy3) and obturator neurons (FITC) in DRGs L3 and L4 were quantified. This provides a control for how well the retrograde labeling worked, with a high cell count yielding a better result. Thus, if the cell count is high, the backfill is more likely to have worked completely, and maximal axons will have reached the RC area for analysis. For all five animals, the cell counts were acceptable, so we were able to analyze those animals. As seen from Table 3, the cell count for the obturator DRG neurons was fairly low for animal 2, with 246 cells. This could be explained by the fact that animal 2 most likely shifted its development of quad and obturator neurons from DRG L3 and L4 to L3 and L2. Thus, we did not see labeled neurons in DRG L4, and the count was slightly lower. Despite this, the obturator afferents were still labeled

well for a normal length of cord, and they had similar percentage of contacts with other animals. Thus, we were able to keep this animal in the data set. As seen from Figure 3, the quad and obturator DRG neurons are co-localized in the same L4 DRG, thus the afferent connectivity with RCs can be compared in the spinal cord.

Figure 2. The distribution of obturator and quad afferents in the RC area of segments L3/L4 around the rostrocaudal axis. Scale bar 200 μ m.

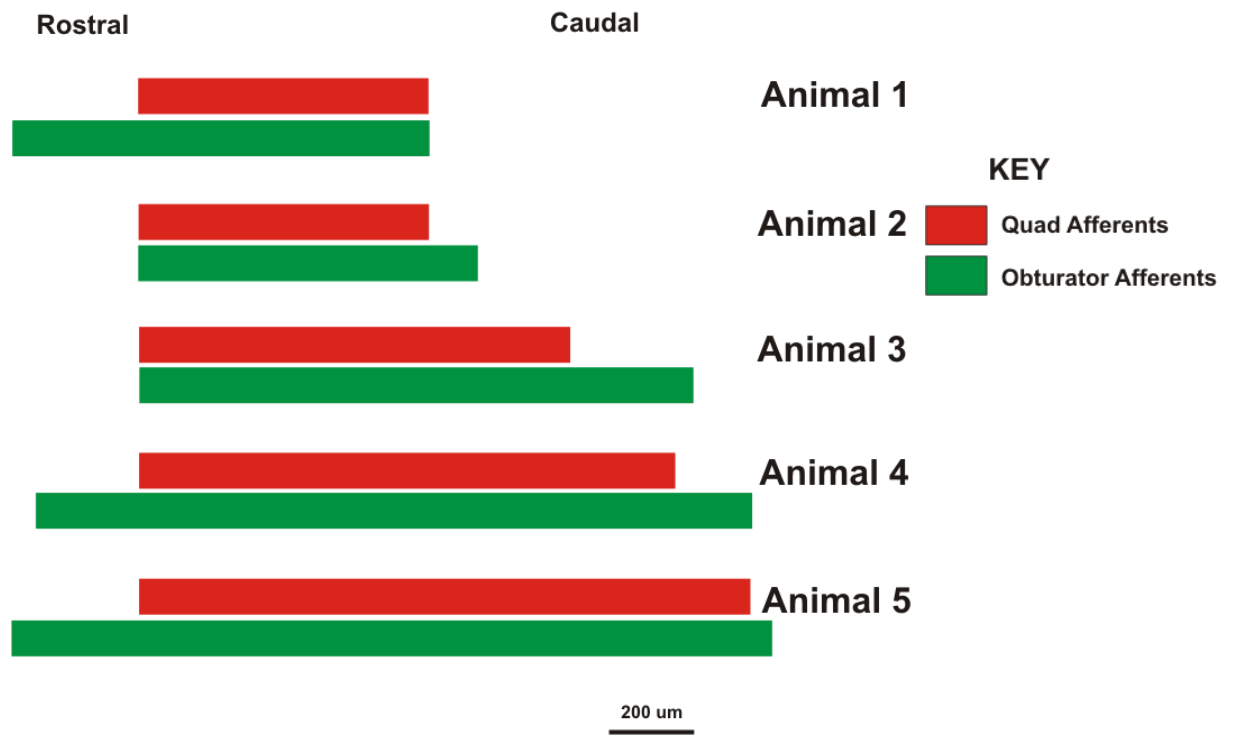
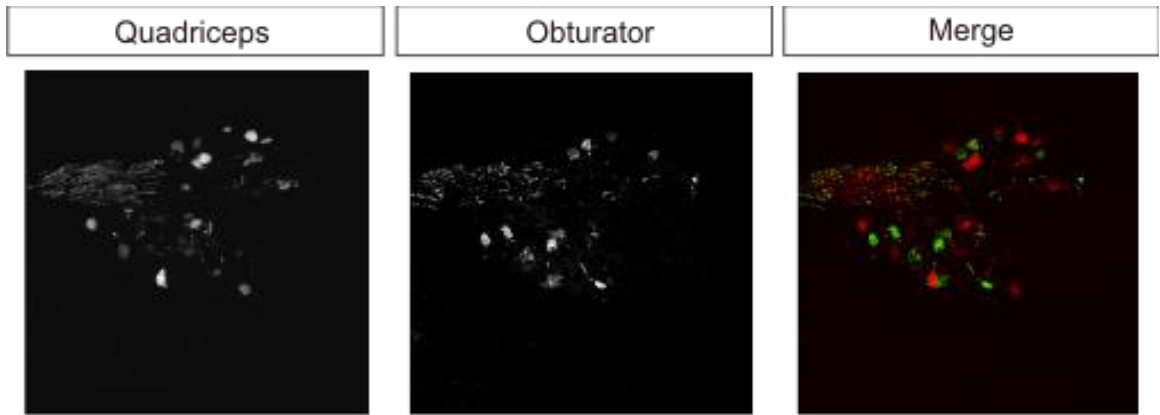


Table 3. Number of total L3/L4 DRG neurons for the quad and obturator nerves in 5 animals, and the average of those 5 animals.

Number of total L3/L4 DRG neurons for the quad and obturator nerves in 5 animals

Animal #	Rhod/Quad # of cells in DRG's L3 and L4	BDA/Obt # of cells in DRG's L3 and L4
1	408	351
2	366	246
3	390	348
4	501	390
5	354	300
Avg	404±17	327±42.9

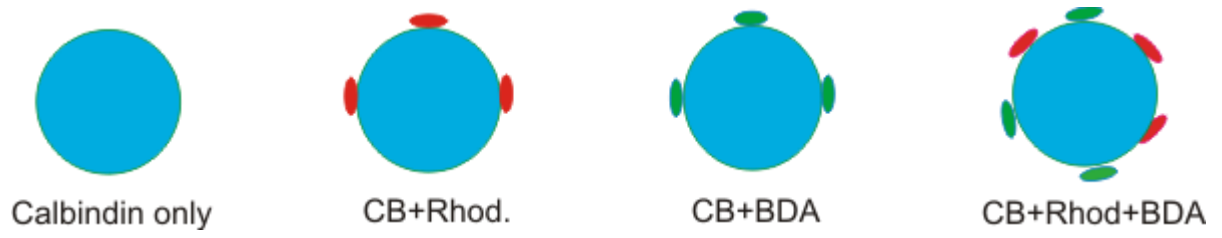
Figure 3. Immunohistochemical image panel of L4 DRG neurons of the quadriceps (red fluorescence) and obturator (green fluorescence) nerves.



High magnification images were used to analyze afferent connectivity on each RC. There were four different possibilities for contact on calbindin + RCs (Fig. 4). First, the cell could have had no contact at all. Second, the cell could have been contacted by the quadriceps nerve (rhodamine) only. Third, the cell could have been contacted by the obturator (BDA) only. Lastly, the cell could have had both quadriceps and obturator contacts. The criterion for inclusion was 1 or more contacts on the soma or dendrite. An example of an image panel of different cells that appear to have only obturator, only quad, or both types of contacts is located in Figure 5. This shows immunohistochemical evidence for both exclusive and convergent inputs to RCs from afferent muscle nerves on subsets of RCs. Even when analysis was restricted to portions of the cord where both quad and obturator afferents were present in the RC area, the average percentage of RCs across five animals with no contacts was $55.6 \pm 4.64\%$ (SEM for $n=5$). The average percentage of RCs with obturator only contact was $20.2 \pm 2.42\%$, the average percentage of RCs with quad only contact was $12.6 \pm 2.09\%$, and the average percentage of RCs with both types of contact was $11.6 \pm 1.69\%$. The general trend on average for connectivity from all the animals is that obturator only contacts are greater (almost 2X) than quad only or both types of contact (Fig. 6 and Table 4). Also, the frequency of quad only contacts are roughly equivalent to a cell having both types of contacts on average. The overall contact data yielded an average of a little more than 1 contact per cell for the first three animals, and animals 4 and 5 having around 1.5 contacts per cell (Table 5). The range was usually around 1-3 contacts per cell, with a cell in animal 5 having the highest number of contacts with 6 (Table 5). Thus,

overall, the average number of contacts per cell was low for all animals examined, and the densities for quad and obturator contacts showed no significant differences.

Figure 4. Types of RC populations.



KEY




-  BDA / Obturator Afferent
-  Calbindin
-  Rhodamine / Quadriceps Afferent

Figure 5. Immunohistochemical image panel showing obturator contacts (green fluorescence overlapping calbindin fluorescence), quad contacts (red fluorescence overlapping calbindin fluorescence), and both types of fluorescence overlapping a calbindin+ RC.

Different Contact Types on Renshaw Cells

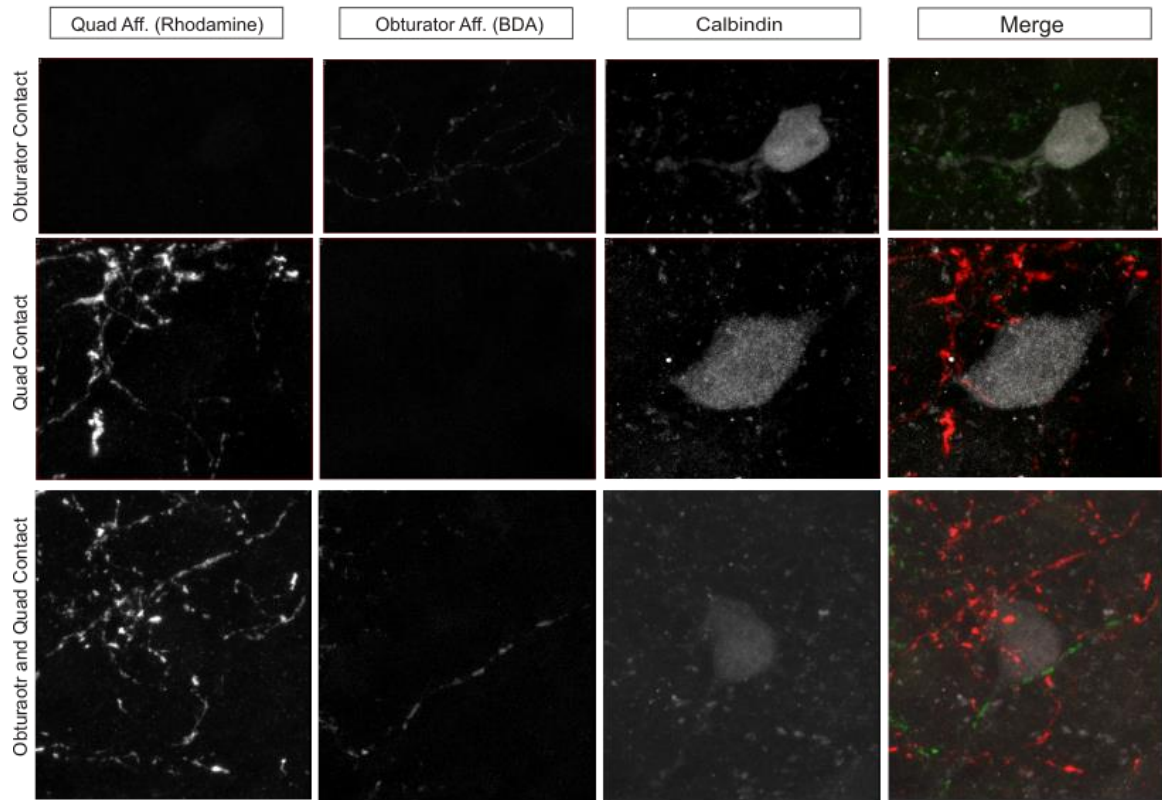


Table 4. Cell Contact Data for obturator and quad nerves in the RC area.

Cell Contact Data for obturator and quad nerves in the RC area.

Animal #	# of RCs	% RCs w/ No Contacts	% RCs w/ only Obt Contacts	% RCs w/ only Quad Contacts	% RCs w/ Both Contacts
1	20	50%	25%	10%	15%
2	36	63%	17%	14%	6%
3	39	67%	15%	8%	10%
4	46	57%	17%	11%	15%
5	64	41%	27%	20%	12%
Average	41	55.6±4.6%	20.2±2.4%	12.6±2.1%	11.6±1.7%

Figure 6. Average percent of RCs with different types of contact for 5 animals.

Average percent of RCs with different types of contact for 5 animals.

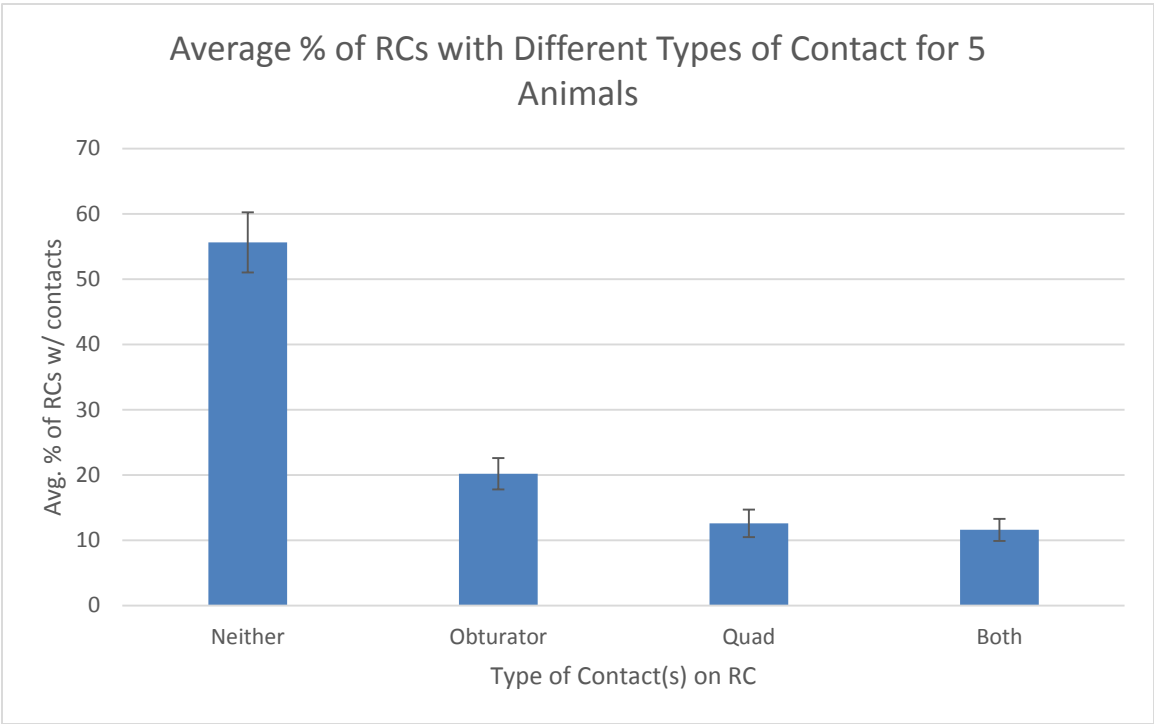


Table 5. Average number of contacts/cell and the range for 5 animals.

Average # of contacts/cell and the range for 5 animals.

	Quad Contacts		Obturator Contacts	
	AVG PER CELL	RANGE	AVG PER CELL	RANGE
Animal 1	1	-	1.3	1-2
Animal 2	1.3	1-3	1.3	1-3
Animal 3	1.3	1-2	1.3	1-2
Animal 4	1.4	1-3	1.5	1-5
Animal 5	1.6	1-6	1.5	1-4

In addition to the above data where analysis was performed when obturator and quad axons were present in the RC area, we also have data from when only the obturator axons were in the RC area. As mentioned previously, depending on the animal, this could have occurred rostrally or caudally to the area where the two types of afferents overlap in the RC area. Approximately $74.8 \pm 8.32\%$ of the cells in these areas did not have contacts. $25.2 \pm 8.32\%$ of cells had at least one obturator contact. The average number of contacts for each cell for animal 1 was 1.3, and the other four animals only had an average of 1 contact per cell. Again, the number of contacts per cell was a low number, and densities were roughly equivalent between quad and obturator contacts.

III. DISCUSSION

This thesis examined the connectivity of Ia afferent neurons with RCs during development by looking at the quadriceps and obturator nerves. Thus, we were able to characterize anatomically the proprioceptive innervation of RCs from newborn mice. We found that there is some bias towards selectivity for the obturator nerve forming connections with RCs over the quad nerve. Specifically, the average percentage of RCs over five animals with obturator only contact was $20.2 \pm 2.42\%$, while the percentage of quad only contacts was $12.6 \pm 2.09\%$. The percentage of RCs that had convergent contacts from both obturator and quad nerves was $11.6 \pm 1.69\%$. Thus, there was some unexpected convergence of Ia afferents on RCs during development. In addition, there was a low average of the number of contacts per cell at this age, with a cell typically having only one or two contacts.

An important point to take into consideration is that when we refer to a cell as being innervated and having a “contact,” we are not absolutely sure it is a true synapse. Our lab has done experiments to address this question: instead of performing a backfill, which was a technique performed in this thesis, an antibody was used against parvalbumin (PV), a specific marker for Ia afferents. In addition, a CB antibody identified RCs, along with location, as was done in this thesis. Finally, a

synaptophysin antibody was utilized. Synaptophysin is a synapse-vesicle anchoring protein, so presumably immunostaining for it helps to visualize synapses. When there was Ia afferent (PV+) contact with a RC (CB+), there was overlap with synaptophysin approximately 74.2% of the time (Ladle Lab, unpublished observations 2015; n=4). Thus, we can come to the conclusion that about three quarters of the contacts in this thesis are likely synapses. This number could also be an underestimation, because at such an early time point in development, a synapse could lack detectable synaptophysin and not be fully mature. The synapse could either have a very weak signal or be too young to acquire the protein, which would cause these synapses to not be detected with the antibody.

We could also determine if the synapse is functional through electrophysiological studies. Mentis et al. (2006) showed that RCs receive inputs from dorsal root sensory primary afferents, and that these inputs represent functional monosynaptic glutamatergic synapses. We could conduct experiments that are more specific, and which involve stimulating either the quad or the obturator nerve and recording from a pool of RCs in L3/L4 to test for a response. In theory, if we tested all the available RCs, we could get a total percentage of RCs that have either quad, obturator, or both types of Ia afferent input.

One of the conclusions from the experiments was that obturator afferents contacted RCs almost twice as frequently as quad afferents. This could be explained several different ways. First, it could be just a transient developmental state. For example, an obturator connection could be seen on a RC at P0, but if examined at P5 this obturator afferent connection may be absent on the RC because this innervation

could have retracted due to CNS plasticity. A similar process is known to occur in the brain with the visual system during postnatal development. During a critical period, if an eye lacks visual input, the synapses from axonal branches that carry this information to the visual cortex will retract, causing blindness in that eye (Antonini and Stryker, 1993). Thus, it is possible that the Ia afferent could withdraw its synapses from the RC at a later period of development due to an activity-dependent mechanism similar to that seen in the visual system.

Another explanation for having more contacts on the obturator nerve has to do with the anatomical locations of the adductor and the quad muscles and their relationship to the amount of RC inhibition their respective motor neuron pools receive. It has been shown that RC inhibition of more ventrally located MNs of proximal musculature is stronger than more dorsally located MNs of distal musculature (Alvarez et al., 2005). Thus, because adductor muscles are more proximally located than quad muscles and presumably their MN pools more ventral, they may have more monosynaptic afferent activity on RCs to produce stronger inhibition of their MN pools.

Differential connectivity between MNs and RCs could be investigated by performing a very similar set of experiments to the ones in this thesis. For example, we could cut the dorsal roots instead of the ventral roots during the dissection. If we still performed the same backfills of the quad and obturator nerves as well as immunostainings for the dextrans and CB, we could visualize the motor axon collaterals that synapse with RCs. We could then identify the number of motor axon collateral contacts on RCs, similar to the analysis of afferent contacts in this thesis.

This would allow us to compare the results from the two different experiments to see if the selectivity pattern is similar or different. If the results show a similar bias for motor axon collateral inputs to RCs (i.e, the obturator nerve), this may help explain our findings. For example, it is possible that obturator RCs mature faster than quad RCs, by forming their inputs at an earlier time period in development. Later on in development, the amount of mature RCs could even out for both quad and obturator cells.

This is one of the reasons it is very important to look at different time points during development in future experiments. Performing these experiments on animals at an older age will allow us to concisely map the selectivity of Ia afferent connections on RCs during development. We will be able to see how this selectivity changes over time and what its final anatomy is in the adult animal. One technical limitation to these experiments is that the backfills performed in this study are not effective after P3. This is because the dextran will not retrogradely travel far enough when the nerve becomes too long in an older animal. We know that by P15, practically all RCs in the lumbar area are contacted by dorsal root sensory primary afferents, but that the number of functional synapses greatly declines in the adult (Mentis et al., 2006). It would be very useful if future methods could find a way to map the connectivity of the quad and obturator nerves in ages up to the P15 animal, when functional synapses are maximized.

One way to do this is use viral tracing methods. We can use a recombinant rabies virus attached to a fluorescent protein (i.e, GFP), to anterogradely label proprioceptive sensory afferents terminating on cells in the ventral horn (Zampieri

et al., 2014). We could inject the rabies virus into the adductors and quad muscles, and 3-6 days after infection we could euthanize the animal and map the afferent connectivity to RCs (Zampieri et al., 2014). For example, if we injected on P9, we could examine the connectivity pattern at approximately P14 or P15.

There are other experiments that could be performed that would explain the bias towards obturator connectivity with RCs. For example, NT3 is a type of neurotrophin, which is important for the differentiation and survival of developing neurons and their circuits (Korsching, 1993). It has been shown that altering NT3 levels in muscle in prenatal transgenic mice changes selective connectivity of proprioceptive afferents with MNs (Wang et al., 2007). We could test the connectivity of proprioceptive afferents with RCs in these transgenic mice that have altered NT3 levels in the obturator and quad muscle, to see if there is a difference with the findings in this thesis. This would allow us to see if and how NT3 levels affect Ia afferent synapses on RCs. Perhaps these muscles express different levels of NT3, which leads to the difference in proprioceptive afferent connectivity with RCs.

Another way to study the development of Ia afferent connections with RCs would be to see if the formation of these connections are activity-dependent. This could be done by blocking synaptic activity through utilization of a conditional knockout allele for *munc18-1*, a protein that is important in vesicle docking and fusion (Rizo and Sudhof, 2002). This allele would be combined with a cre-recombinase allele only expressed in proprioceptive afferents (Parvalbumin-cre), and Ia afferent synaptic transmission would be blocked (Dallman and Ladle, 2013). We could then use this as a tool to study Ia afferent connectivity during

development in the absence of activity at the level of the synapse, and these results could be compared with that of a wild-type animal. Although the recurrent inhibition circuit doesn't require synaptic activity to develop properly (Alvarez et al., 2013), it would be interesting to see if Ia afferent connections with RCs are affected by a lack of synaptic activity.

Another outcome not predicted by our initial hypothesis is that approximately 10% of the RCs on average had convergent contacts. We would expect there to be no dually innervated RCs because the quad and adductor muscles are not related in any way. Thus, in a very structured and functional system, we would expect obturator and quad afferents to contact separate pools of RCs. However, early on in development, the process seems to be more random than this. Stimulating a dorsal root in the rat activates a greater variety of MNs in earlier development than later stages, hinting at less specificity of connections which will later become a more focused system (Saito, 1979). Similarly, it is quite possible that these dually innervated RCs have inappropriate connections that will dissipate with later development and locomotion. This may represent a sort of activity-dependent plasticity, similar to the process mentioned above that occurs with development of the visual system. Another possibility is that one synapse may overpower or silence the other synapse, in effect making only one input functional. Alternatively, the RCs with convergent contacts could represent the population that show contacts on the analysis, but one of the afferents does not actually form a synapse. We could test for this by performing the synaptophysin staining mentioned earlier in the discussion. Synaptophysin could have been viewed because we have 4 channels available on

our confocal microscope. This would have allowed us to count a contact only when synaptophysin was co-localized with CB and rhodamine or BDA, ensuring a more accurate possibility of a true synapse. However, this was not performed in the thesis because it would make analysis too difficult due to the abundance of synaptophysin staining in the cord along with possible bleaching issues. In addition, as mentioned previously this was performed as a separate project, which allows us to say with confidence what percentage of contacts are actually synapses.

In our study, the majority of cells ($55.6 \pm 4.6\%$) had neither obturator nor quad contacts. This could be explained by the fact that only at P15 are 100% of RCs contacted by a monosynaptic afferent in the lumbar region (Mentis et al., 2006). At an early stage in development right after birth (P0/P1), it would follow that this circuitry would not be fully mature and thus many RCs would not be innervated yet. Specifically, 60-64% of mouse RCs received contacts from dorsal root axons at birth (Mentis et al., 2006). This would make approximately 40% of RCs lacking afferent contact at birth in the Mentis study, compared to our 56%. A way to explain this discrepancy is that there are nerves that innervate other muscles besides the quad and adductors, which send their sensory information to DRG L4. For example, the tibial nerve and fibular nerve innervate muscles in the legs, and they send sensory afferents to the L4 spinal segment. Thus, it is quite possible that some of the RCs that did not receive putative synapses from either quad or obturator nerves could be innervated by the tibial or fibular nerves.

One purpose for these monosynaptic Ia afferent inputs to RCs could be to produce a generalized feedforward inhibition mechanism. An example of

feedforward inhibition occurs in the medial prefrontal cortex of the brain, which is activated by local interneurons that receive powerful excitation from basolateral amygdala pyramidal neurons (Dilgen et al., 2013). This allows emotional information from the amygdala to impact our decision-making skills in the prefrontal cortex. Likewise, the possible feed-forward inhibition mechanism at work in this thesis would allow Ia afferents to excite RCs which would subsequently inhibit MNs, largely affecting motor output.

Clearly if RCs were not functioning properly, this feed-forward inhibition on MNs would also be impaired. One hypothesized way diminished RC function occurs is in disease states, such as ALS. In early stages (presymptomatic) of ALS, there is a loss of motor axon synapses with RCs, which affects the recurrent inhibition circuit (Wootz et al., 2013). This would indirectly decrease the amount of inhibition to MNs by way of RCs and eventually lead to MN degeneration, presumably affecting motor output. If decreased excitation of RCs is one of the causative factors of ALS, it is quite possible that monosynaptic Ia afferent inputs to RCs could also be affected. Without this input, we would also have decreased excitation of RCs leading to less inhibition of MNs. An experiment to conduct would be to utilize a SOD1 transgenic mouse (ALS mouse model) and perform the same protocol that was used in this thesis. This would allow us to see if glutamatergic synapses on RCs are affected by the experimental form of ALS at a developmental stage well before symptom onset.

To conclude, we have discovered information pertaining to the proprioceptive afferent connectivity of different muscle nerves with RCs during development in a mouse model. Specifically, we found that the Ia afferent

component of the obturator nerve contacts RCs at a frequency almost two times greater than the quad nerve at P0/P1. Also contrary to our hypothesis is the finding that there is a population of RCs that receive convergent contacts from both quad and obturator nerves at the same age. Finally, over half the RCs do not receive input from either the quad or obturator nerves. In order to obtain more information regarding the reasons for the results in this thesis, many future experiments will need to be performed.

IV. BIBLIOGRAPHY

- Alvarez, F. J., Benito-Gonzalez, A., and Siembab, V. C. (2013). Principles of interneuron development learned from Renshaw cells and the motoneuron recurrent inhibitory circuit. *Annals of the New York Academy of Sciences*, 1279, 22-31.
- Alvarez, F. J., and Fyffe, R. E. (2007). The continuing case for the Renshaw cell. *The Journal of Physiology*, 584(1), 31-45.
- Alvarez, F. J., Jonas, P. C., Sapir, T., Hartley, R., Berrocal, M. C., Geiman, E. J., Todd, A. J., and Goulding, M. (2005). Postnatal phenotype and localization of spinal cord V1 derived interneurons. *Journal of Comparative Neurology*, 493(2), 177-192.
- Arber, S., Ladle, D. R., Lin, J. H., Frank, E., and Jessell, T. M. (2000). ETS gene Er81 controls the formation of functional connections between Group Ia sensory afferents and motor neurons. *Cell*, 101(5), 485-498.
- Antonini, A., and Stryker, M. P. (1993). Rapid remodeling of axonal arbors in the visual cortex. *Science*, 260(5115), 1819-21.
- Benito-Gonzalez, A., and Alvarez, F. J. (2012). Renshaw cells and Ia inhibitory interneurons are generated at different times from p1 progenitors and differentiate shortly after exiting the cell cycle. *Journal of Neuroscience*, 32(4), 1156-1170.
- Bhumbra, G. S., Bannatyne, B. A., Watanabe, M., Todd, A. J., Maxwell, D. J., and Beato, M. (2014). The recurrent case for the Renshaw cell. *The Journal of Neuroscience*, 34(38), 12919-12932.
- Chen, A. I., de Nooij, J. C., and Jessel, T. M. (2006). Graded activity of transcription factor Runx3 specifies the laminar termination pattern of sensory axons in the developing spinal cord. *Neuron*, 49, 395-408.
- Chen, H. H., Hippenmeyer, S., Arber, S., and Frank, E. (2003). Development of the monosynaptic stretch reflex circuit. *Current Opinion in Neurobiology*, 13, 96-102.

- Chen, H. H., Tourtellotte, W. G., and Frank, E. (2002). Muscle spindle-derived neurotrophin 3 regulates synaptic connectivity between muscle sensory and motor neurons. *Journal of Neuroscience*, 22, 3512-3519.
- Dallman, M. A., and Ladle, D. R. (2013). Quantitative analysis of locomotor defects in neonatal mice lacking proprioceptive feedback. *Physiology & Behavior*, 120, 97-105.
- de Nooij, J. C., Doobar, S., and Jessel, T. M. (2013). Etv1 inactivation reveals proprioceptor subclasses that reflect the level of NT3 expression in muscle targets. *Neuron*, 77, 1055-1068.
- Dilgen, J., Tejada, H. A., and O'Donnell, P. (2013). Amygdala inputs drive feedforward inhibition in the medial prefrontal cortex. *Journal of Neurophysiology*, 101(1), 221-229.
- Eccles, J. C., Fatt, P., and Koketsu, K. (1954). Cholinergic and inhibitory synapses in a pathway from motor-axon collaterals to motoneurons. *Journal of Physiology (London)*, 126, 524-562.
- Korsching, S. (1993). The neurotrophic factor concept: A reexamination. *Journal of Neuroscience*, 13, 2739-2748.
- Kucera, J., Fan, G., Jaenisch, R., Linnarsson, S., and Ernfors, P. (1995). Dependence of developing group Ia afferents on neurotrophin-3. *The Journal of Comparative Neurology*, 363 (2), 307-320.
- Mentis, G. Z., Siembab, V. C., Zerda, R., O'donovan, M. J., and Alvarez, F. J. (2006). Primary afferent synapses on developing and adult Renshaw cells. *Journal of Neuroscience*, 26(51), 13297-13310.
- Nishimaru, H., Koganezawa, T., Kakizaki, M., Ebihara, T., and Yanagawa, Y. (2010). Inhibitory synaptic modulation of Renshaw cell activity in the lumbar spinal cord of neonatal mice. *Journal of Neurophysiology*, 103, 3437-3447.
- Patel, T. D., Kramer, I., Kucera, J., Niederkofler, V., Jessell, T. M., Arber, S., and Snider, W. D. (2003). Peripheral NT3 signaling is required for ETS protein expression and central patterning of proprioceptive sensory afferents. *Neuron*, 38(3), 403-416.
- Renshaw, B. (1946). Central effects of centripetal impulses in axons of spinal central roots. *Journal of Neurophysiology*, 9, 191-204.
- Rizo, J., and Südhof, T.C. (2002). Snares and munc18 in synaptic vesicle fusion. *Nature Reviews Neuroscience*, 3(8), 641-53.

- Saito, K. (1979). Development of spinal reflexes in the rat fetus studied in vitro. *Journal of Physiology (London)*, 294, 581-594.
- Sapir, T., Geiman, E. J., Wang, Z., Velasquez, T., Mitsui, S., Yoshihara, Y., Frank, E., Alvarez, F. J., and Goulding, M. (2004). Pax6 and Engrailed 1 regulate two distinct aspects of Renshaw cell development. *The Journal of Neuroscience*, 24(5), 1255-1264.
- Sengul, G., Puchalski, R. B., and Watson, C. (2012). Cytoarchitecture of the spinal cord of the postnatal (P4) mouse. *The Anatomical Record (Hoboken)*, 295(5), 837-45.
- Siembab, V. C., Smith, C. A., Zagoraïou, L., Berrocal, M. C., Mentis, G. Z., and Alvarez, F. J. (2010). Target selection of proprioceptive and motor axon synapses on neonatal V1-derived Ia inhibitory interneurons and Renshaw cells. *Journal of Comparative Neurology*, 518(23), 4675-4701.
- Stam, F. J., Hendricks, T. J., Zhang, J., Geiman, E. J., Francius, C., Labosky, P. A., Clotman, F., and Goulding, M. (2012). Renshaw cell interneuron specialization is controlled by a temporally restricted transcription factor program. *Development*, 139(1), 179-190.
- Wang, Z., Li, L., Goulding, M., and Frank, E. (2008). Early postnatal development of reciprocal Ia inhibition in the murine spinal cord. *Journal of Neurophysiology*, 100(1), 185-196.
- Wang, Z., Li, L., Taylor, M. D., Wright, D. E., and Frank, E. (2007). Prenatal exposure to elevated NT3 disrupts synaptic selectivity in the spinal cord. *Journal of Neuroscience*, 27, 3686-3694.
- Williams, E. R., and Baker, S. N. (2009). Renshaw cell recurrent inhibition improves physiological tremor by reducing corticomuscular coupling at 10 Hz. *The Journal of Neuroscience*, 29(20), 6616-6624.
- Wootz, H., Fitz-Simons-Kantamneni, E., Larhammar, M., Rotterman, T. M., Enjin, A., Patra, E., van Zundert, B., Kullander, K., Alvarez, F. J. (2013). Alterations in the motor neuron-Renshaw cell circuit in the Sod1 mouse model. *Journal of Comparative Neurology*, 521(7), 1449-1469.
- Zampieri, N., Jessel, T. M., and Murray, A. J. (2014). Mapping sensory circuits by anterograde trans-synaptic transfer of recombinant rabies virus. *Neuron*, 81(4), 766-778.
- Zhang, L., Schmidt, R. E., Yan, Q., and Snider, W. D. (1994). NGF and NT-3 have differing effects on the growth of dorsal root axons in developing mammalian spinal cord. *Journal of Neuroscience*, 14, 5187-5201.